Rev. Mexicana Astron. Astrof. **12**. 393-398 (1986)

AUTOMATIC IDENTIFICATION OF FAINT IMAGES ON THE ESO/SRC SKY ATLAS

R. Chan, P. S. Pellegrini and L. N. da Costa

Department of Astronomy, CNPq-Observatório Nacional
Brasil

ABSTRACT. This paper describes the automatic image classification system developed at the Observatório Nacional (ON). The system is currently being used in photometric studies of moderately distant clusters of galaxies utilizing the on-film copies of the ESO/SRC Sky Atlas.

I. INTRODUCTION

In recent years there has been a renewed interest in photometric studies of clusters of galaxies, especially at different cosmological look-back times. This interest has been primarily motivated by the results of Butcher and Oemler (1978), which suggested that a significant evolution in the galactic content of rich clusters has occured quite recently. The importance of this so-called Butcher-Oemler effect is enormous since it would provide an unique opportunity of observing an evolutionary process in clusters in progress. Moreover the development of new techniques to analyze large areas of photographic plates, digitized with computer-controlled microdensitometers, opens up new perspectives for systematic studies of a large number of clusters at different epochs.

In this paper we show that the vast material available in the form of film copies of the ESO (B) and ESO/SRC (J) and (R) Sky Atlas can be used to study the photometric properties of moderately distant clusters of galaxies. For this purpose we have developed an algorithm for automatic image detection and star-galaxy classification. In section II we briefly outline this algorithm, the performance of our image classification and the photometric quality obtained using the on-film copies of the ESO and ESO/SRC Atlas. As an illustration, in section III we derive some general properties of the cluster Abell 1146 utilizing the sample of galaxies produced by our automated classification system.

II. DETECTION, CLASSIFICATION AND PHOTOMETRY OF IMAGES

The on-film copies were scanned utilizing the PDS 1010A microdensitometer of the ON in Rio de Janeiro. All scans were made using a 10 micra (0".67) square aperture which, after some experimentation, seemed to be the best compromise between image resolution and limiting isophote, taking into account the characteristics of the available material.

The system for automatic classification of faint images consists of routines for sky determination, object detection and star-galaxy separation. The sky background is determined by fitting a two dimensional fifth order polynomial to the density measurements of the digitized area and by eliminating the large positive residuals. This procedure is repeated until an approximately symmetric distribution of residuals is obtained. The algorithm for object detection is similar to other systems developed in the past (e.g. Tyson and Jarvis 1979). It processes the data sequentially, comparing the density of each pixel in a scan line to a set threshold level above the local sky density. Using the 10 micra aperture, the threshold used corresponds to the isophotal limits $\mu_B = 24.5$ mag arc sec^{-2} and $\mu_J = 25.5$ mag arc sec^{-2} for the ESO (B) and ESO/SRC (J) films, respectively. Contiguous pixels above the threshold are grouped together to represent a probable object. An image is considered complete when no more pixels are added to it after processing an entire line. However, it is only considered a real object if the total number of pixels is greater than a chosen minimum. All density readings associated to the object are then converted to intensity and subtracted by the local sky intensity. The characteristic curves for the ESO/SRC (J) films are obtained from the step wedges available in each field, while for the ESO (B) films a mean curve is used, similar to that derived by de Carvalho et al. (1985). Finally, various parameters are computed for the detected objects, such as: the center of the image weighted by the intensity distribution; the isophotal magnitude; total number of pixels and area of the image; central surface brightness; mean surface brightness; major and minor diameters; position angle; characteristic radii, r_n weighted by the two-dimensional image light distribution, similar to those defined by Kron (1980).

In order to select the most adequate classifier for our purposes, we have implemented into our classification algorithm several criteria discussed in the past involving different combinations of image parameters: mean surface brightness versus magnitude (Godwin and Peach 1977); central surface brightness versus magnitude (Jarvis and Tyson 1980); log (area) versus magnitude (MacGillivray 1981); log (r_n) versus magnitude, equivalent to the selection criteria used by Kron (1980). Experiments with the data have shown that the

lassifier based on the radius r_1 is the most satisfactory for the plate scale f the Schmidt films, separating more clearly the domains of stars and galaxies figure 1).

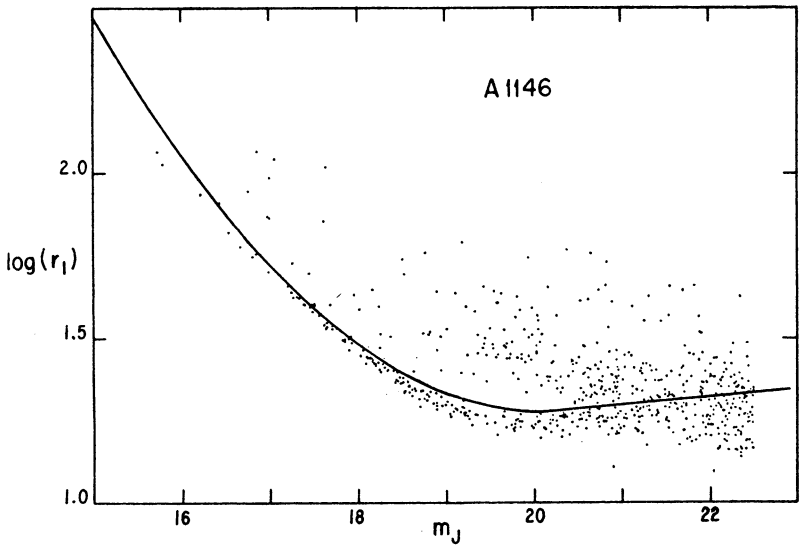

Fig. 1 The radius r_1 plotted against the J magnitude for the sample of objects on the field of A1146

ıe upper envelope of the stellar sequence, which curves at the bright end due ɔ image saturation, defines the borderline between the star and galaxy ɔpulations. As indicated by Kron (1980) this method is powerful because r_1 ɜ, by definition, independent of the magnitude for unsaturated stars. Images ɔove the plotted line can be assumed to be galaxies but for very faint objects ıe separation becomes less clear because of the low resolution of the Schmidt ilms. This prevents a reliable classification beyond $m_J \sim 21.0$ on the ɜO/SRC (J) films and $m_B \sim 20.0$ on the ESO (B) films and brightwards, the ɔmpleteness of the galaxy sample is almost 100%. These limiting values were ɜrived by comparing our classification with the deeper galaxy sample of Carter ıd Godwin (1979). To minimize the effect of overlapped images and to eliminate ļate defects we also reanalyze the data using a higher threshold and visually ıspect the classified images. The purity of the final sample, as defined by ıtchins (1982), is usually high and typically only 10% of the galaxies have ıcorrect magnitudes due to merged images.

The photometric quality of our data was tested comparing our ɜophotal magnitudes with the (pseudo) total magnitudes obtained by Carter and ɔdwin (1979) for the cluster A1146 (figure 2). This comparison shows no

indications of systematic errors in our magnitudes and that for galaxies brighter than m_J=21.0 our isophotal magnitudes are close to the total magnitudes. A similar analysis for the ESO (B) films yelds m_B=20.0 as this limiting magnitude. From the comparison between the two data sets we can also estimate that the photometric accuracy is < 0.2, in both cases.

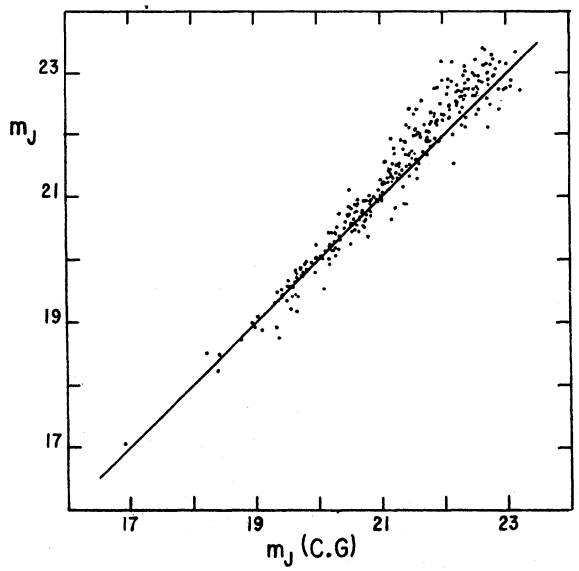

Fig. 2 Galaxy isophotal J magnitude plotted against (pseudo) total magnitudes of Carter and Godwin (1979).

III. CLUSTER PROPERTIES

The sample of galaxies brighter than m_J = 21.0, identified by our classifier, is used here to derive some properties of the cluster A1146. The space distribution for these galaxies is shown in figure 3, covering an area approximately the same as that shown by Carter and Godwin (1979) for a deeper sample. For m_J < 21.0 the discrepancy between the two samples is of only three objects.

In figure 4 we show the projected radial density distribution obtaine from galaxy counts in equal width (0.15 Mpc) rings around the cluster center. Also shown is the projected isothermal distribution fitted to the counts, yelding a core radius r_c = 0.21 Mpc. It is interesting to note the presence of a small hump in the counts at $\sim$ 0.7 Mpc, which may be indicative of sub-clustering.

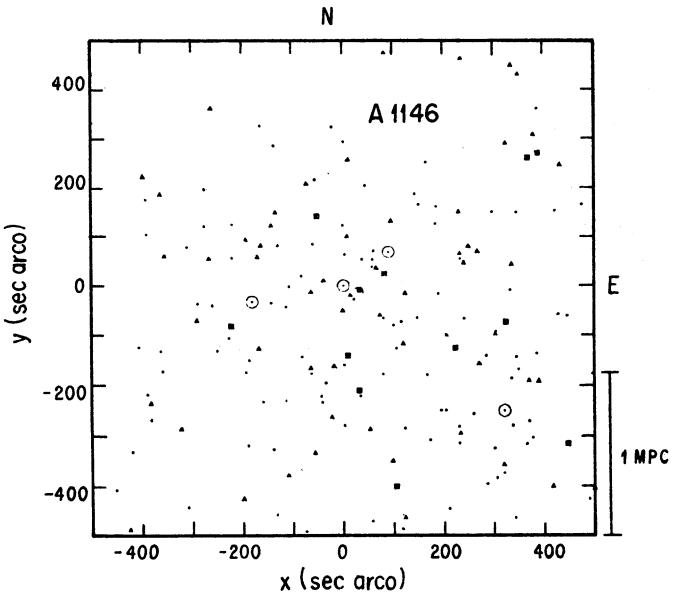

Fig. 3 Distribution of galaxies with $m_J < 21.0$ in the cluster A1146. The different symbols denote 1 mag intervals relative to the brightest galaxy. The symbols (θ), (■), (▲), (•) are in a increasing order of magnitude.

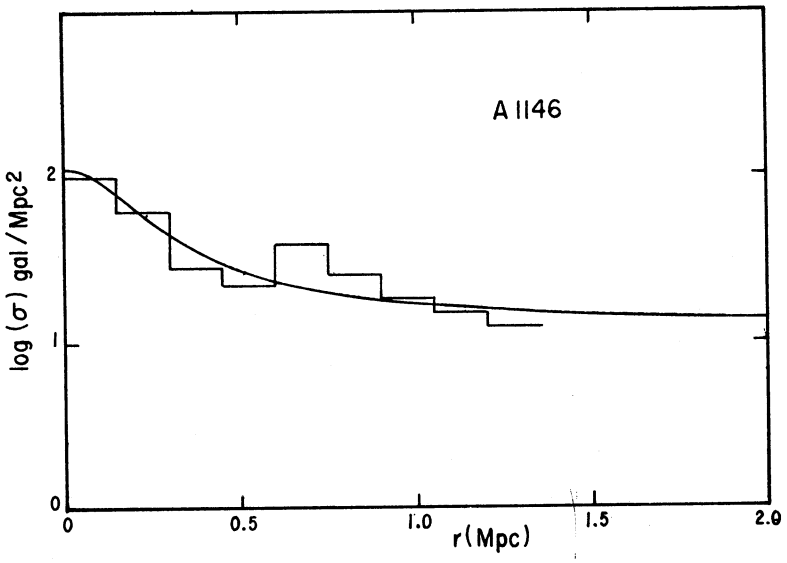

Fig. 4 Radial density distribution in cluster A1146. The histogram is the observed distribution and the solid line represents the fit with the isothermal model.

The differential cluster luminosity function is shown in figure 5. It was determined subtracting the field luminosity function, determined in an adjoining area of the cluster, from the cluster region luminosity function. In the plot we also show the best-fit of a Schechter function described by $M_J^*=-21.12$ and $\alpha=1.25$, very close to the standard values.

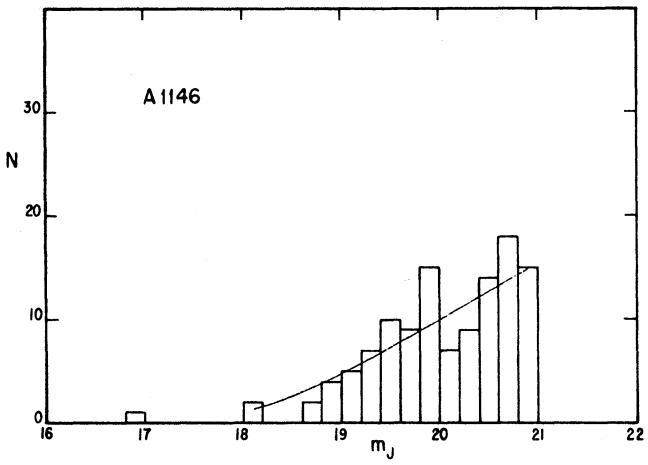

Fig. 5 The differential luminosity function of A1146.

The results obtained so far are promising, demonstrating that photometric studies of clusters of galaxies in a wide range of redshifts can be adequately carried out utilizing the on-film copies of the ESO and ESO/SRC Sky Atlas. Based on these preliminary evaluations we expect to investigate several clusters in the redshift range 0.1 to 0.2.

REFERENCES

Butcher, H., and Oemler, A. 1978, Ap. J., 226, 559.
Butchins, S.A. 1982, Astr. and Ap. 109, 360.
Carter, D., and Godwin, J. G. 1979, M.N.R.A.S., 187, 711.
de Carvalho. R.R., da Costa, L.N., and Pellegrini, P.S. 1985, to be published in Astr. and Ap..
Godwin, J.G., and Peach, J.V. 1977, M.N.R.A.S., 181, 323.
Jarvis, J.F., and Tyson, J.A. 1981, Astr. J., 86, 476.
Kron. R.G. 1980, Ap. J. Suppl., 43, 305.
MacGillivray, H.T. 1981, in Astronomical Photography, ed. by J.L. Heudier and M. E. Sim (Nice: Centre Nationale de la Recherche Scientifique and Institut Nationale d'Astronomie et de Geophysique), P. 277.
Tyson, J.A., and Jarvis, J.F. 1979, Ap. J. Lett., 230, L153.

L.N. da Costa, R. Chan, and P.S. Pellegrini: Department of Astronomy, CNPq-Observatório Nacional, Rua General Bruce 586, São Cristóvão 20921, Rio de Janeiro RJ Brasil.